Social learning moderates the tradeoffs between efficiency, stability, and equity in group foraging

Ze-Xu Li^a, M. Amin Rahimian^b,* and Lei Fang^a,c,d*

- ^a Civil and Environmental Engineering, University of Pittsburgh
- ^b Department of Industrial Engineering, University of Pittsburgh
- Department of Mechanical Engineering and Materials Science, University of Pittsburgh
 Department of Bioengineering, University of Pittsburgh
 - * To whom correspondence should be addressed; email: {rahimian,lei.fang}@pitt.edu.

Social learning shapes collective search by influencing how individuals use peer information. Empirical and computational studies show that optimal information sharing, neither too localized nor too diffuse, can improve resource detection and group coordination. Building on these insights, we develop a randomized search model integrating social learning with area-restricted search (ARS) to examine how communication distance affects collective foraging outcomes. Our model incorporates three behavioral modes: exploration, exploitation, and targeted walk, to evaluate how groups balance local exploitation with global exploration. These modes are controlled by one key parameter ρ that balances exploration and exploitation between the collective. We examine how communication distance affects group efficiency (η) , its temporal variability (σ) , and equity in resource distribution (ϵ) . We identified an intriguing tradeoff between the three outcomes. As $\rho \to 0$, the agents explore the search field independently, leading to maximum collective exploration. With increasing ρ , agents prioritize exploiting patches that other members of the group identify before engaging in their own explorations. The η is maximized while σ is minimized at interior values of ρ that effectively balance exploration and exploitation. As ρ increases to the maximum range in the search field, the equality among individuals is maximized, but this comes at the cost of lower η and σ values. In addition, we introduce negative rewards to assess how social learning aids in risk mitigation and observe that search efficiency is optimized at lower values of ρ with increasing number of negative targets or magnitude of negative rewards. Surprisingly, we can also use "fake" negative rewards to improve the efficiency of collective search by focusing the collective exploration effort away from empty regions of the search field. Our results clarify the trade-offs that shape adaptive collective behavior in complex environments.

Search is a critical behavior for mobile foragers, such as albatrosses [1], marine predators [2, 3], and hunter-gatherers [4, 5, 6], who must secure random and often sparsely distributed food resources in complex environments. Active search mode demands substantial allocation of limited energy budget and increases exposure to predators and environmental hazards. These challenges underscore the need for efficient search strategies that balance energy expenditure with resource acquisition.

A widely studied strategy for efficient search is the Lévy walk [1, 2, 3], a movement pattern that is closely related to but physically distinct from the mathematical construct of the Lévy flight. Both describe step lengths drawn from a power law distribution $P(l) \sim l^{-\mu}$ (1 < $\mu \leq 3$), which produces clusters of short displacements interspersed with occasional very long steps, forming fractal patterns without a characteristic scale. In the idealized Lévy flight, the steps are instantaneous, allowing arbitrarily long jumps in zero time, whereas a Lévy walk couples each step length to the time required to traverse it at finite speed, making it the appropriate model for real organisms. Early empirical work often used the term Lévy flight when the measured trajectories were, in fact, finite-speed Lévy walk. In their seminal work [1], Viswanathan et al. (1996) test the Lévy foraging hypothesis with flight patterns of the wandering albatross. They posit that Lévy foraging represents an evolved, optimal strategy for searching in uncertain environments, a claim bolstered by Viswanathan et al. (1999), who mathematically demonstrate that powerlaw step length statistics can outperform other movement patterns, such as Brownian motion, when targets are sparsely distributed [7]. However, early enthusiasm was tempered by critiques, notably Edwards et al. [8], who expose statistical missteps in attributing the power-law scaling to some species, prompting the need for more rigorous methodologies. With improved analysis, the Lévy walk-like search has been confirmed in various systems, including T cells in the brain [9], swarming bacteria [10, 11], honeybees [12], aquatic marine predators [2, 3], and even hunter-gatherers [4].

Research on the Lévy foraging hypothesis suggests that animals searching for sparse and randomly distributed resources may benefit from movement patterns that approximate Lévy walks [7, 13, 14]. More recent work on intermittent, two-stage search shows that real foragers rarely follow a purely memoryless Lévy process. Food encounters often trigger area-restricted search (ARS) behavior, in which individuals switch from rapid, wide-ranging motion to slower, more tortuous paths near a resource patch [15, 16, 17, 18]. Modeling studies demonstrate that such encounter-driven ARS can outperform idealized Lévy walks by reducing the overall search time [16], increasing the encounter rates, and lowering the risk of starvation [15], especially when resources are scattered in patches.

In nature, many organisms search for food items collectively for survival. When an animal is not successful in locating food sources, it can instead locate other distant group members who are successful and join them. Collective search is a ubiquitous phenomenon observed across different species [19, 20, 21, 22], which harnesses the power of group dynamics to improve efficiency within environments where resources are often scarce, highly clustered, or ephemeral [23].

The efficiency of collective problem solving, however, depends critically on how infor-

mation flows through social networks. Lazer & Friedman [24] demonstrated that network topology regulates the balance between exploration and exploitation; Mason & Watts [25] provided experimental evidence that efficient communication networks enhance group learning; and Becker et al. [26] revealed that patterns of social influence alter collective accuracy in "wisdom-of-crowds" tasks. Within this framework, our communication-range parameter ρ serves as a spatial analogue of network connectivity, enabling direct examination of how information-exchange density regulates group performance. By linking ecological models of foraging with network-theoretic approaches to collective intelligence, we bridge behavioral ecology and social-network science, providing a mechanistic foundation for how connectivity mediates exploration-exploitation trade-offs.

At the heart of these dynamics lies social learning-the process by which individuals acquire and use information from others to guide behavior [27, 28]. The role of social learning in the collective search is multifaceted as it mediates how individuals process and act on information from their peers, profoundly affecting both individual and group outcomes. Empirical work on Mongolian gazelles, for instance, shows that vocal communication over intermediate distances optimizes foraging efficiency by guiding group members toward rich resource patches while avoiding the pitfalls of overly localized or excessively diffuse information sharing [29]. Similarly, computational models reveal that probabilistic interactions, in which foragers selectively move toward sites of successful peers, can generate scale-free movement patterns similar to Lévy walks, enhancing search efficiency in heterogeneous landscapes [27]. Two trade-offs have been found, exploration versus exploitation, and individual search versus social learning can drive the coexistence of explorative and exploitative strategies within groups. However, excessive copying of others leads to suboptimal group efficiency unless it is mitigated by adaptive heuristics, such as area-restricted search [31].

Here, we use a deterministic (range-based) social learning model integrated with arearestricted search (ARS) to investigate the optimal communication distance at which groups can
balance local exploitation and global exploration to maximize foraging efficiency across diverse
target environments. In our model, we define three behavioral strategies: exploration, exploitation, and targeted walk to examine how the communication distance influences the efficiency of
collective search. In addition, we investigate its impact on temporal patterns of efficiency and
equitable resource distribution between individuals. Furthermore, we incorporated negative targets into our model to elucidate the effects of social learning on risk mitigation in foraging
environments.

In this paper, we model group foraging by N_A agents that start at random locations within the domain and follow a Lévy walk with $\mu=1.1$, executing an explorative strategy with longer steps; see Materials and Methods for details of the Lévy walk model with two modes of exploration and exploitation. Upon detecting a target, an agent will collect it and send a social signal sharing the location of the detected target with all other agents within a radius of ρ , which is the social learning parameter that determines the range of response to a social signal. Simultaneously, the agent that has just collected a target adjusts its search strategy from explorative to

exploitative, changing μ from 1.1 to 3 to perform an area-restricted search. When an agent does not find any new targets within radius R of its last collected target, it ends its area-restricted search and reverts to the explorative search strategy, changing its μ from 3 to 1.1 (Fig. 1).

Agents who have not received social signals (out of the social learning range ρ) or are conducting an area-restricted search continue to perform their own search strategy independently. In contrast, agents within the social learning range performing an explorative search ($\mu=1.1$) will stop their random walk and move towards the location where the social signal was sent (targeted walk). However, agents who are already doing a targeted walk will compare the distances between the two different destinations and choose the closest one. During the targeted walk, if agents encounter a new target, they will terminate the targeted walk and initiate an area-restricted search in its vicinity.

Results

We simulate our group foraging model by varying the social learning range from $\rho=0$ to $\rho=0.7$, which is the largest social learning range in our domain, using a periodic boundary condition. Considering that the targets are limited and nonregenerative, search efficiency will definitely drop as more targets are depleted. Each simulation will end when 30% of the targets have been collected [30, 31]. We also vary the number of patches, keeping the total number of targets across all patches fixed at 6000. Furthermore, we introduce negative targets, conceptualized as risks encountered by agents during the search, that negatively impact search efficiency. When an agent encounters a negative target, it can also send a social signal to inform agents within a radius ρ of the presence of the negative target. Upon approaching known negative targets, agents exhibit active avoidance behaviors.

Efficiency

The group efficiency, defined as $\eta = N_{collected}/N_{positive}T$, quantifies the rate at which agents collect positive targets. Here, $N_{collected}$ and $N_{positive}$ are the number of targets collected by agents and the total number of targets within the domain, respectively. T is the total search time. As the social learning range (ρ) increases, it first increases and then decreases, with an optimal ρ that yields the highest efficiency. (Fig. 2A). This phenomenon is robust across different numbers of patches, whether we fix the total number of targets or the number of targets per patch (see Supplementary Fig. 4). It can also be observed for target distributions with $\beta=1.1$ (see Supplementary Fig. 2) and $\beta=3$ (see Supplementary Fig. 3), as well as different group sizes when N=10 (see Supplementary Fig. 5). It is not surprising because Garg et al. [30] have revealed two trade-offs: the trade-off between exploitation and exploration in individual search controlled by the power-law exponent μ , and the trade-off between individual search and social learning modulated by selectivity parameter. However, our clearer definition of exploration and exploitation can better explain the occurrence of the optimal ρ .

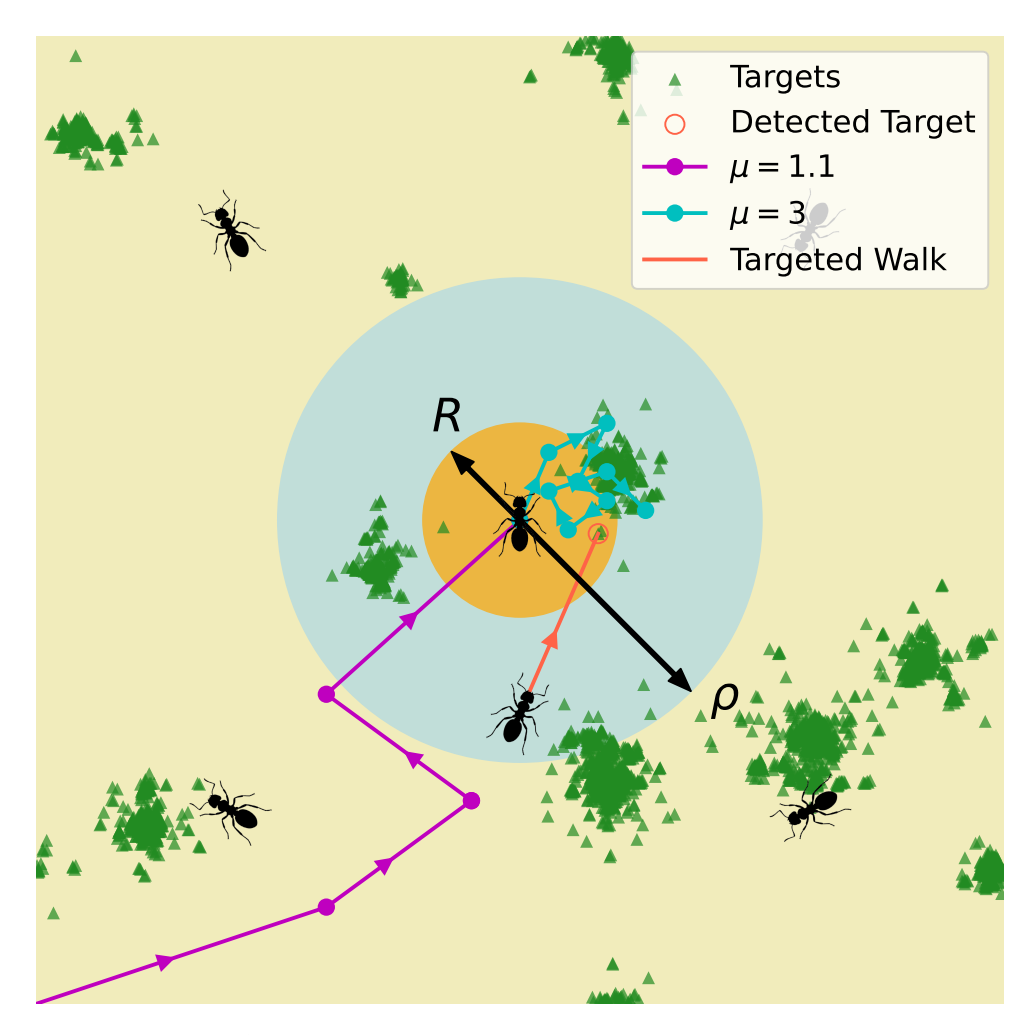


Figure 1: A schematic of the collective search model. Agents begin by performing independent Lévy walks with $\mu=1.1$ (exploration, shown in purple) until they detect a target. Upon detection, the agent ceases social learning and switches to a Lévy walk with $\mu=3$ (exploitation, shown in blue) within a circular region of radius R centered at the detected target, which is updated over time. Meanwhile, a social signal emitted by this agent attracts other agents within a region of radius ρ to perform targeted walk towards the detected target (shown in orange). Agents outside this region do not receive the social signal and maintain their search mode.

Agents in our model exhibit three modes: Levy work with $\mu=1.1$, Levy work with $\mu=3$, and targeted walks triggered by social learning. We interpret $\mu=1.1$ mode as global exploration, $\mu=3$ mode as area restricted exploitation, and the targeted walk as the operational cost associated with exploitation. Agents can adaptively switch between the three modes as needed. We measure the time spent on each mode, as shown in Fig. 2B. When $\rho=0$ (no social learning), targeted walks do not occur, and agents search independently, spending approximately 90% of their time on exploration. After encountering a target, an agent shifts from exploration

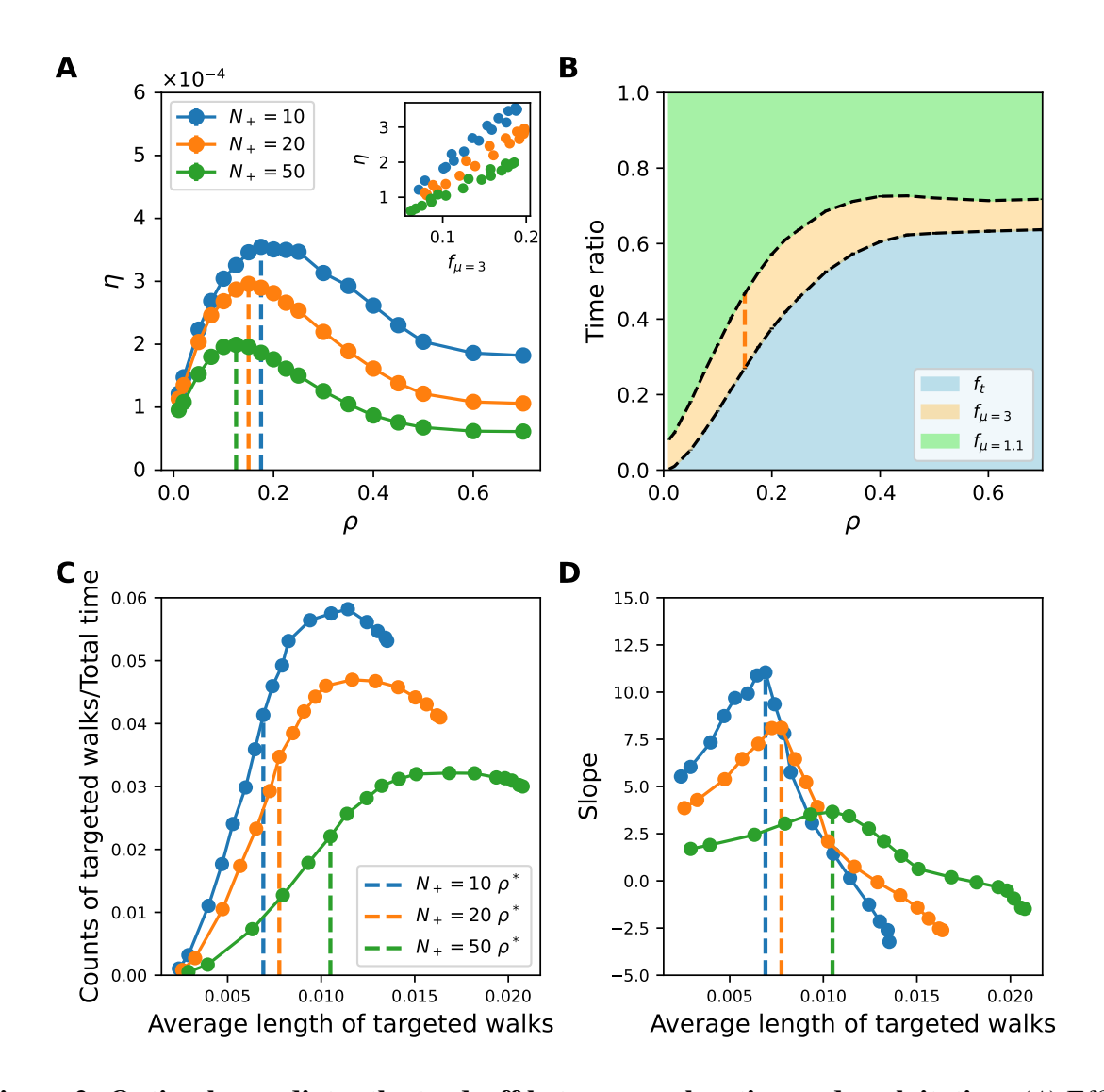


Figure 2: Optimal ρ mediates the tradeoff between exploration and exploitation. (A) Efficiency versus ρ for a fixed number of agents ($N_A=50$) and three numbers of positive patches ($N_+=10;20;50$). The total number of targets is fixed at 6000 with $\beta=2$. Error bars denote 95% confidence intervals but are too small to be visible. The inset shows that efficiency increases monotonically with the $f_{\mu=3}$. (B) Average time fractions spent in three behaviors for the $N_+=10$ case in (A); the optimal ρ aligns with the social-learning regime where agents spend the largest fraction of time exploiting targets ($\mu=3$). (C) Counts of targeted walks, normalized by total time (benefit), plotted against their average length (cost). (D) Slope of the curve in (C) as a function of targeted-walk length, showing that the highest benefit-to-cost ratio coincides with the optimal ρ .

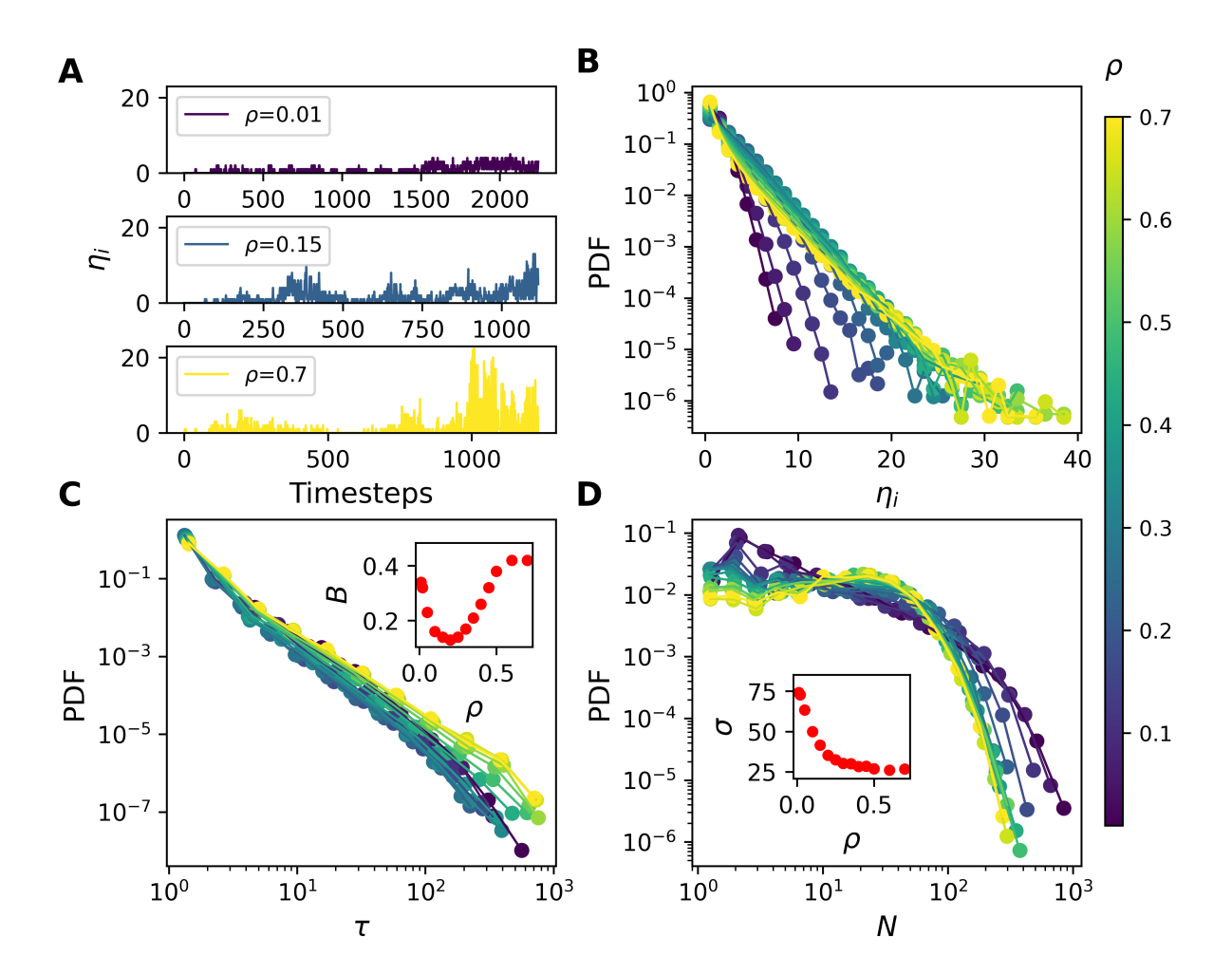


Figure 3: Heterogeneity across time and space. (A) Time variation of instantaneous efficiency η_i with $\rho=0.01$, $\rho=0.15$, and $\rho=0.7$ (showing one case). η_i represents the number of collected targets per time step. (B) Probability density function (PDF) of η_i indicating that low $\rho \leq 0.2$ limits η_i due to less social learning, while higher ρ (0.2 < ρ < 0.5) allows η_i to reach greater values with an exponential distribution. For $\rho \geq 0.5$, the proportion of medium η_i values decreases, though η_i can achieve higher values with a heavy-tail distribution. (C) PDF of inter-event time, defining an event as when the instantaneous efficiency $\eta_i \geq 1$. The inset figure illustrates the variation of the burstiness parameter B with ρ . The optimal ρ corresponds to the lowest B, indicating a steady intake of resources and, consequently, a minimal starvation time. (D) PDF of number of collected targets by each agent, with an inset indicating that the standard deviation (representing equity) decreases as ρ increases. All data is based on a scenario with 50 agents and $N_+ = 10$.

to exploitation, which contributes to the remaining 10% of time spent on exploitation. As ρ in-

creases, targeted walks become more prevalent, triggering greater exploitation. Consequently, the time ratio of exploration decreases as ρ rises. At the optimal ρ , the time ratio of exploitation reaches its maximum. This reflects an elegant balance between exploration and exploitation: enough exploitation sustains high current efficiency, while just enough exploration continually discovers new patches, preserving future opportunities and, in turn, overall efficiency. As ρ increases further, targeted walks become more prevalent. However, the time ratio of exploitation decreases, indicating that an excessively high proportion of targeted walks leads to redundant search effort and reduces the exploitation ratio. This occurs because the number of targets is limited in each patch. When social signals attract most of the agents to a detected target, earlyarriving agents can still collect targets, whereas late-arriving agents who travel for extended periods can only collect a few targets. Additionally, the remaining targets may be insufficient to support sustainable exploitation, causing late-arriving agents to revert to exploration soon. In other words, the social signal breaks the exploration of those late-arriving agents (far from the social signal) and lets them restart exploration from a region where most of the targets are consumed. Thus, an excessively large ρ , causes a high proportion of targeted walks, raises the cost and reduces the benefits of exploitation, disrupts the exploration process, and forces agents to explore regions where most targets are already consumed, thereby diminishing efficiency.

From Fig. 2A, we observe that the optimal ρ increases as the number of patches, N_+ , decreases, as exploiting a single patch becomes more critical than exploring new ones in this scenario. Conversely, when targets are distributed across a larger number of patches, agents must identify more patches to collect 30% of the targets. Additionally, efficiency is higher in scenarios with fewer patches, as agents spend less time searching for new patches. Furthermore, we plot efficiency, η , as a function of $f_{\mu=3}$ in the inset of Fig. 2A, demonstrating that η is positively correlated with $f_{\mu=3}$. The slopes of the η - $f_{\mu=3}$ curves vary due to differences in the number of targets per patch. A larger number of targets per patch (the case with $N_+=10$) leads to a larger slope of η - $f_{\mu=3}$, meaning that increasing the time ratio of exploitation becomes more beneficial.

To investigate the role of social learning and the resulting targeted walk, we construct a phase diagram in 2C, plotting the counts of targeted walks normalized to the total time in each case, against the averaged length of targeted walks. In this diagram, a higher count of targeted walks signifies increased interaction with social signals, which promotes exploitation and enhances efficiency. Conversely, a larger average length of targeted walks represents high cost, as it is the distance agents must travel before they can begin detecting a resource, which reduces overall efficiency. The slope of the curves in this phase diagram, therefore, represents the ratio of benefits to costs, specifically the gain from increased exploitation per unit of cost. Based on this, we hypothesize that the point where the slope of each curve reaches its maximum corresponds to the most efficient scenario. At this point, the benefit gained from targeted walks increases most rapidly relative to their cost. To verify this hypothesis, we compute the derivative of the curves from the phase diagram as shown in Fig. 2D, which reveals the slope. From the figure, a maximum value of the derivative represents the most efficient scenario. This derivative is smoothed using a Gaussian filter with $\sigma = 1$ to reduce the noise.

Timeseries characteristic and equality

We select $\rho=0.01$, $\rho=0.2$, and $\rho=0.7$ to illustrate the temporal variation in the number of targets collected by all agents per time step (Fig. 3A), which we define as instantaneous efficiency, η_i . Here, the number of agents is set at $N_A=50$, and the domain contains 10 patches, each with 600 targets. When $\rho=0.01$, agents search nearly independently and share minimal information about target locations, resulting in a limited η_i that remains low for an extended period. This occurs because the number of agents visiting a patch limits the number of collected targets per timestep. As ρ increases to $\rho=0.15$ (the optimal ρ), η_i reaches higher values, indicating agents can cooperate effectively to collect targets in one patch. As ρ increases further, such as $\rho=0.7$, targeted walks attract more agents to exploit the same patch, which increases instantaneous η_i further. However, this high efficiency cannot be sustained, as excessive agent exploitation rapidly depletes resources, leaving little exploration. As a consequence, η_i rapidly decays to a low level. Upon the total consumption of the existing target, agents require time to explore new target patches, during which η_i drops to zero. Thus, a larger ρ results in a bursty instantaneous efficiency.

To highlight the burstiness of η_i , we plot its probability density functions (PDFs), as shown in Fig. 3B. The PDF reveals that a larger ρ increases the proportion of higher η_i values, resulting from social learning and agent aggregation. To further reveal the bursty pattern existing in the timeseries of instantaneous efficiency, we use the burstiness parameter introduced by Goh and Barabási [32]. Here, we defined an event as occurring when η_i exceeds 0, while the interevent time τ represents the starvation time during which agents do not collect any targets. The burstiness parameter is quantified by $B \equiv (\sigma_\tau - m_\tau)/(\sigma_\tau + m_\tau)$, where m_τ and τ_m are the mean and standard deviation of τ , respectively. Fig. 3C shows the PDFs of interevent times, where cases with high and low ρ exhibit a larger proportion of starvation time, reflecting greater burstiness and leading to lower efficiency. The inset in Fig. 3C plots the burstiness parameter B as a function of ρ , where ρ values with lower B correspond to the optimal ρ . Thus, the analysis of the time series and the derived burstiness provides another perspective on the optimal ρ , which not only exhibits the highest efficiency but also steady intake of resources and reduced burstiness in starvation time.

In addition, we measure individual efficiency and examine its variation within a group of agents. Using the same parameter values, we plot the PDFs of the number of targets collected by each agent, as shown in Fig. 3D. From the low- ρ regime to the high- ρ regime, the shape of PDF becomes flatter with increasing probability of medium N values, and the range of the number of targets collected by each agent narrows, indicating that the benefits from targets are distributed more equally among agents. However, while a larger ρ enhances both equity and efficiency, an excessively large ρ increases equity but reduces efficiency and increases burstiness.

Negative targets

Social learning enables agents to aggregate and collect targets, thereby increasing efficiency. In nature, however, prey foraging for food face multifaceted risks, including predation, environ-

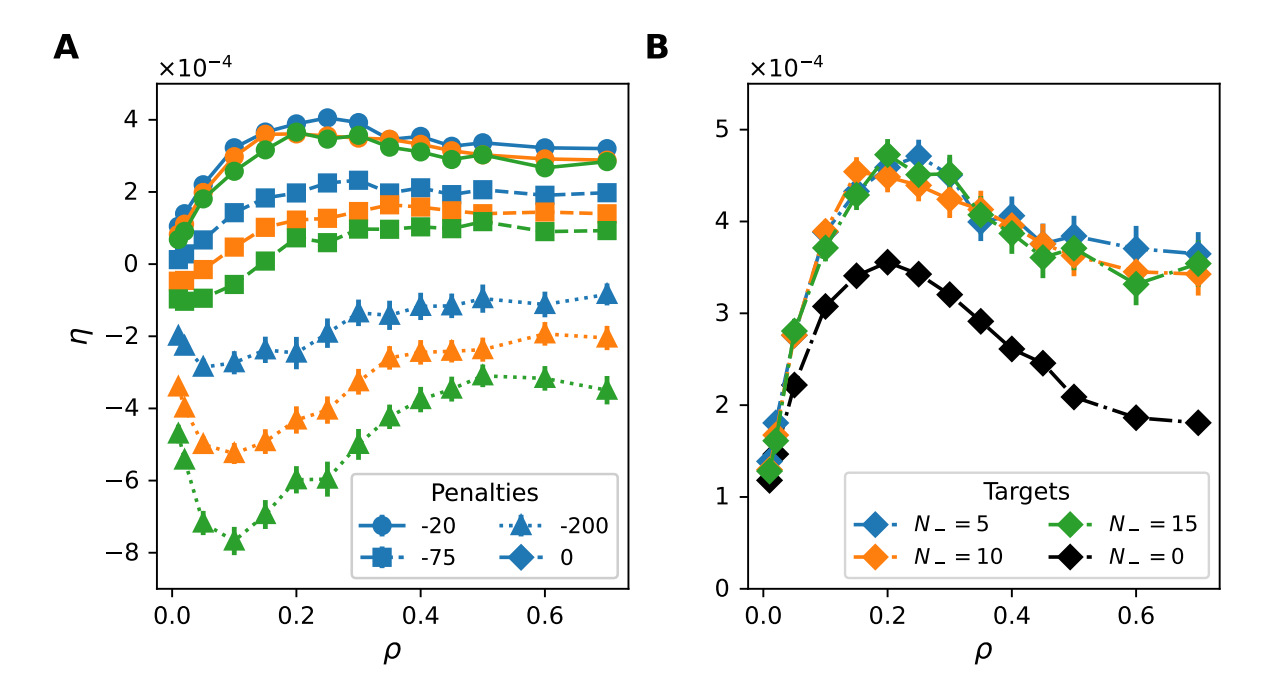


Figure 4: Negative patches changes optimal ρ and may improve efficiency (A) Efficiency as a function of density ρ for three penalty coefficients (P=-20, P=-75, and P=-200). Colors indicate the number of negative patches ($N_-=5$, 10, and 15), with the number of positive patches fixed at $N_+=10$. The total number of targets and negative targets in the domain is fixed at 6000. The controlling parameter for the target distribution is $\beta=2$ and the simulated group size is 50. The optimal ρ increases as the penalty increases, indicating avoiding negative patches is more important than searching for targets. (B) Ignoring the penalty, scenarios containing negative patches achieve higher efficiency than those with only positive patches, indicating that adding randomly distributed fake negative patches can enhance overall efficiency.

mental hazards, and resource depletion, which can compromise their survival and efficiency. If agents can not only share information about the locations of beneficial resources, but also the existing risks in the domain, will the potential risks affect the results and conclusions in our collective search model with social learning? To model this, we introduce negative targets that penalize agents, while allowing agents to share information about risks, enabling others to actively avoid these negative targets after receiving social signals (**See Methods**). We then examine the influence of these risks on our model.

We fixed the total number of positive and negative targets at 6000 each. The number of positive patches, N_+ , is set to 10. We then vary the number of negative patches, N_- , to change the ratio of positive patches to negative patches. To calculate the efficiency, we measure the number of collected positive targets ($N_{collect+}$) and negative targets ($N_{collect-}$), accounting for

penalties from negative targets, using the formula $\eta = (N_{collect+} + P \cdot N_{collect-})/(N_{positive} \cdot T)$. Here, P is the penalty coefficient, representing the strength of the penalty imposed by each negative target. As P varies from -20 to -200, the increased penalties reduce efficiency, leading to a higher optimal ρ . Because larger penalized coefficients change the major concern for maximizing efficiency, shifts from rapidly collecting more positive targets to avoiding encountering negative targets, which necessitate greater ρ , although it will diminish the efficiency contributed from positive targets.

For the same penalty coefficient P, we observe that the differences in efficiency curves between cases with varying numbers of negative patches increase as the penalty rises. This occurs because a higher number of negative patches allows agents to detect more negative targets, which in turn leads to a greater overall penalty.

From Fig. 4B, where the penalty for detecting negative targets is set to zero, we surprisingly find that randomly distributed negative patches significantly increase efficiency. This occurs because detected negative targets from randomly generated patches exclude certain regions of the domain, thereby constraining the area that agents explore, which reduces the time required to explore a new patch. This is true even though the patch centers are independently generated. The improvement in efficiency from adding negative patches does not appear to depend on the number of negative patches.

Discussion

The presented work advances the understanding of collective foraging by demonstrating that the social learning range ρ —the distance over which individuals respond to social signals—acts as a crucial tuning parameter that regulates a complex interplay between efficiency (η), temporal stability, and equitable resource distribution in group foraging. Our central finding is that optimal foraging efficiency occurs at intermediate values of ρ , offering a unified, mechanistic explanation for patterns observed across disparate biological and computational systems [29, 27, 30, 31]. This work advances beyond previous literature by explicitly quantifying the multi-faceted costs and benefits of social information sharing in dynamic and risk-laden environments.

In network terms, ρ defines the effective connectivity radius: as ρ increases, each agent's social neighborhood expands, approximating a denser communication graph. When $\rho \to 0$, the network fragments into isolated nodes; when $\rho \to 0.7$, it approaches full connectivity. Thus, the observed non-monotonic dependence of efficiency on ρ parallels prior findings that intermediate network density maximizes collective performance [33, 34].

Our finding of an optimal intermediate range for information sharing confirms a recurring theme in the collective search and foraging literature. The peak efficiency observed at intermediate ρ aligns with the theoretical finding in Mongolian gazelles [29], where acoustic communication over intermediate distance optimizes search efficiency. This pattern of optimal intermediate communication also mirrors findings from Deborah Gordon's work on harvester ants,

where restrained signaling maintains efficient colony foraging [35, 36, 37]. Our framework generalizes these empirical observations by explicitly linking ρ to the balance of three distinct behavioral modes: global exploration ($\mu=1.1$), local exploitation ($\mu=3$), and targeted walk. Furthermore, the model offer a clearer mechanistic explanation for why non-optimal range fails. When ρ is too small, agents search nearly independently, leading to maximum exploration but minimum cooperation, akin to a purely individual search. This is consistent with finding that insufficient information sharing hampers successful searches [38, 39, 40]. On the other hand, if ρ is too large, excessive targeted walks occur, leading to redundant search effort and premature depletion of local patches. This highlights a cost of social learning that suppresses the crucial simultaneous discovery of multiple patches [27], and effect observed in empirical studies of bird foraging [41, 42].

Our model incorporates adaptive switches between two Lèvy walk modes ($\mu=1.1$ and $\mu=3$), providing a composite search strategy that advances beyond traditional Lèvy models. Pure, memoryless Lèvy walk, while optimal for sparse, randomly distributed targets [7, 2, 43], often fail to account for the adaptive behavior of real foragers. Our model supports the notion that encounter-conditional heuristics, such as Area-Restricted Search (ARS) triggered by a successful encounter, are often superior to idealized Lèvy walks, especially in patch environments [15]. Moreover, the targeted walk mode, absent from individual ARS models, serves as a socially-mediated exploitation mechanism. Our analysis of the targeted walk's benefit-to-cost ratio provides a quantitative link between a social behavior (joining successful peers) and the resulting gain in efficiency, clearly demonstrating that the highest benefit-to-cost ratio coincides with the optimal ρ .

Prior theoretical studies on collective foraging primarily focused on maximizing search efficiency [39, 44, 27, 30, 31]. Our work provides a missing, multifaceted perspective by explicitly quantifying the trade-offs ρ creates with temporal stability and equity of resource intake. The impact of ρ on the burstiness parameter and instantaneous efficiency reveals a crucial trade-off between maximizing average efficiency and maintaining a steady resource stream. While high ρ can lead to short, intense bursts of instantaneous efficiency, it ultimately results in a high burstiness and increased starvation time. This bursty, highly unstable dynamics is consistent with "herding" and maladaptive informational cascades observed in human social learning experiments [45]. The lowest burstiness (maximal stability) is found at the same intermediate ρ that optimizes η . This suggests that optimal efficiency is intrinsically linked to stability in dynamic foraging environments. Social learning is a "double-edged sword", but our model shows the optimal range manages this risk, mitigating the tendency toward rapid, inflexible, and ultimately unsustainable resource exploitation that plagues systems with high social dependence [45]. The mechanism underlying the optimal intermediate ρ can also be interpreted through the lens of transient diversity-the temporary coexistence of heterogeneous behaviors or information states. When ρ is small, diversity persists but coordination is limited; when ρ is large, information homogenizes too quickly, leading to premature convergence on local optima. Intermediate ρ maintains transient diversity long enough to explore alternative solutions before consensus, echoing a general principle found across formal models of collective problem solving [46].

By measuring the distribution of collected targets per agent, our work directly addresses the producer-scrounger paradigm from a spatial and kinematic perspective [27, 47]. Our results demonstrate that increasing ρ flattens the distribution of collected targets among agents, thereby increasing equity. However, this gain in equity at high ρ comes at the cost of overall lower efficiency and increased instability, as the collective engages in redundant search efforts. Our findings provide an individual-level mechanism for the group-size effects seen in real systems: In the *Australomisidia ergandros* spider, larger group sizes increase scrounger-type frequency and decrease producer frequency [47]. For human social learning, rates of copying increases with group size [45]. These experimental observations has been verified by our model. The time ratio of the targeted walk reaches 0.6 in a group of 50 agents, which is significantly higher than 0.4 in a group of 10 agents, as shown in Supplementary Figure 5, with the same target distribution.

Our incorporation of negative targets (risks) into the collective search domain introduces a novel dimension of realism to foraging models. The optimal ρ adpatively shift from intermediate to higher as the penalty magnitude increases. This is a key insight: when risks are severe, the group's priority shifts from maximizing immediate resource collection to prioritizing risk avoidance through wider social information gathering. Based on that, we surprisingly found that adding randomly distributed "fake" negative patches (with zero penalty) significantly increased overall efficiency. This novel emergent mechanism arises because the negative social signals effectively constrain the search space, focusing the collective exploration effort away from empty regions, leading to faster patch discovery. This suggests a completely new principle for designing cooperative search algorithms in robotics and swarms [48, 49, 44].

In summary, this work presents a unified mechanistic framework that integrates efficiency, stability, equity, and risk sensitivity within collective search. By demonstrating that these competing objectives are simultaneously optimized at intermediate social learning ranges, we reveal a general principle underlying collective adaptation. The results reconcile diverse empirical observations—from ants and gazelles to human groups—and provide a testable foundation for designing resilient, self-organized systems in both biological and engineered collectives.

Methods

Search space and target distribution

The search space is represented by a two-dimensional grid (1000×1000) on a square with a unit length side (d=1), so that each cell of the grid has dimensions $d_{min} \times d_{min}$, where $d_{min} = 10^{-3}$. The total number of targets N_T , is grouped into N_+ positive target patches or N_- negative patches. The patches are initialized at $N_+ + N_-$ random locations, and additional targets are placed around previously placed resources at distance d_T , according to the probability of $P(d_T) = C d_T^{-\beta}$, where $d_{min} \leq d_T \leq L$, and C is the normalization constant that ensures the probability distribution sums to 1, $C = (1 - \beta)/(L^{1-\beta} - (d_{min})^{1-\beta})$. β controls the pattern

of clustering of targets, where $\beta \to 1$ resembles a uniform distribution, and $\beta \to 3$ generates a tightly clustered target distribution. The resources in the model are destructive; that is, they are removed from the environment after being detected by agents.

Lévy walks with exploration and exploitation modes

The individual search strategy of the agents is based on the Lévy walk, in which the moving orientation of the agents is chosen randomly and the distance (d) is determined by the following distribution, $P(d) = Cd^{-\mu}$, where $d_{min} \leq d \leq L$, and μ is the power-law exponent. C is a normalization constant, $C = (1-\mu)/(L^{1-\mu}-(d_{min})^{1-\mu})$. The Lévy exponent μ modulates the individual search behavior between shorter steps and longer steps. As in $\mu \to 1$, the agents move in a longer step with an explorative strategy, while $\mu \to 3$. During each timestep, agents move in fixed step sizes of $d_{min} = 10^{-3}$ to cover a total step length d, which is sampled from a probability distribution. Each step corresponds to a constant speed of d_{min} per timestep, and larger values of d require more time steps to complete. At each timestep, each agent searches within a radius $r = d_{min}$ and collects one target if it exists in the range.

Effects of detected negative target

When an agent detects a negative target, it shares the target's location with other agents within a radius of ρ around itself. The interaction between a detected target and agents aware of its location is modeled using an exponentially decaying function, $l=0.002e^{-50d}$, where d represents the distance between the agent and the detected target, and l is the repulsive step length directed outward from the detected target to the agent's current position. This function decays rapidly, and l falls below the minimum step length d_{min} when d>R, ensuring that l has minimal effect on agents far from the detected target and allows agents to avoid the region around the negative target within a radius R. This repulsive step is superimposed on the agents' movement, which follows a Lévy walk or targeted walk, thereby altering the agents' moving direction while maintaining their constant speed of d_{min} per timestep.

Variance reduction

Considering that our model is based on a random walk, which introduces randomness to the statistics, we use the same set of target distributions for cases with different ρ to reduce variance. To minimize the errorbar with a 95% confidence interval, we run 2000 cases for each ρ .

Code and Data availability

All python scripts used to generate the figures and reproduce the simulation results in this paper are openly available on our GitHub repository: https://github.com/LoneStar97/social-learning-

Acknowledgements

Research was sponsored by the DEVCOM Analysis Center and was accomplished under Contract Number W911QX-23-D0002. The views and conclusions contained in this document are those of the authors and should not be interpreted as representing the official policies, either expressed or implied, of the DEVCOM Analysis Center or the U.S. Government. The U.S. Government is authorized to reproduce and distribute reprints for Government purposes notwithstanding any copyright notation herein.

This research was supported in part by the University of Pittsburgh Center for Research Computing, RRID:SCR_022735, through the resources provided. Specifically, this work used the HTC cluster, which is supported by NIH award number S10OD028483.

References

- [1] G. M. Viswanathan, *et al.*, Lévy flight search patterns of wandering albatrosses, *Nature* **381**, 413 (1996).
- [2] D. W. Sims, *et al.*, Scaling laws of marine predator search behaviour, *Nature* **451**, 1098 (2008).
- [3] D. W. Sims, N. E. Humphries, R. W. Bradford, B. D. Bruce, Lévy flight and brownian search patterns of a free-ranging predator reflect different prey field characteristics, *Journal of Animal Ecology* **81**, 432 (2012).
- [4] D. A. Raichlen, *et al.*, Evidence of lévy walk foraging patterns in human hunter–gatherers, *Proceedings of the National Academy of Sciences* **111**, 728 (2014).
- [5] V. V. Venkataraman, T. S. Kraft, N. J. Dominy, K. M. Endicott, Hunter-gatherer residential mobility and the marginal value of rainforest patches, *Proceedings of the National academy of Sciences* **114**, 3097 (2017).
- [6] L. Pacheco-Cobos, *et al.*, Nahua mushroom gatherers use area-restricted search strategies that conform to marginal value theorem predictions, *Proceedings of the National Academy of Sciences* **116**, 10339 (2019).
- [7] G. M. Viswanathan, *et al.*, Optimizing the success of random searches, *nature* **401**, 911 (1999).
- [8] A. M. Edwards, *et al.*, Revisiting lévy flight search patterns of wandering albatrosses, bumblebees and deer, *Nature* **449**, 1044 (2007).

- [9] T. H. Harris, *et al.*, Generalized lévy walks and the role of chemokines in migration of effector cd8+ t cells, *Nature* **486**, 545 (2012).
- [10] G. Ariel, *et al.*, Swarming bacteria migrate by lévy walk, *Nature Communications* **6**, 8396 (2015).
- [11] G. Ariel, A. Be'er, A. Reynolds, Chaotic model for lévy walks in swarming bacteria, *Physical review letters* **118**, 228102 (2017).
- [12] A. M. Reynolds, *et al.*, Displaced honey bees perform optimal scale-free search flights, *Ecology* **88**, 1955 (2007).
- [13] G. M. Viswanathan, E. Raposo, M. Da Luz, Lévy flights and superdiffusion in the context of biological encounters and random searches, *Physics of Life Reviews* **5**, 133 (2008).
- [14] N. E. Humphries, D. W. Sims, Optimal foraging strategies: Lévy walks balance searching and patch exploitation under a very broad range of conditions, *Journal of Theoretical Biology* **358**, 179 (2014).
- [15] C. Ross, L. Pacheco-Cobos, B. Winterhalder, A general model of forager search: Adaptive encounter-conditional heuristics outperform lévy flights in the search for patchily distributed prey, *Journal of Theoretical Biology* 455, 357 (2018).
- [16] O. Bénichou, C. Loverdo, M. Moreau, R. Voituriez, Two-dimensional intermittent search processes: An alternative to lévy flight strategies, *Physical Review E-Statistical*, *Nonlinear, and Soft Matter Physics* **74**, 020102 (2006).
- [17] S. Benhamou, J. Collet, Ultimate failure of the lévy foraging hypothesis: Two-scale searching strategies outperform scale-free ones even when prey are scarce and cryptic, *Journal of Theoretical Biology* **387**, 221 (2015).
- [18] G. H. Pyke, Understanding movements of organisms: it's time to abandon the lévy foraging hypothesis, *Methods in Ecology and Evolution* **6**, 1 (2015).
- [19] C. Barnard, R. Sibly, Producers and scroungers: a general model and its application to captive flocks of house sparrows, *Animal Behaviour* **29**, 543 (1981).
- [20] C. Detrain, J.-L. Deneubourg, Collective decision-making and foraging patterns in ants and honeybees, *Advances in Insect Physiology* **35**, 123 (2008).
- [21] F. Ginelli, *et al.*, Intermittent collective dynamics emerge from conflicting imperatives in sheep herds, *Proceedings of the National Academy of Sciences* **112**, 12729 (2015).
- [22] L. Gómez-Nava, R. Bon, F. Peruani, Intermittent collective motion in sheep results from alternating the role of leader and follower, *Nature Physics* **18**, 1494 (2022).

- [23] L.-A. Giraldeau, T. Caraco, *Social Foraging Theory* (Princeton University Press, 2018).
- [24] D. Lazer, A. Friedman, The network structure of exploration and exploitation, *Administrative science quarterly* **52**, 667 (2007).
- [25] W. Mason, D. J. Watts, Collaborative learning in networks, *Proceedings of the National Academy of Sciences* **109**, 764 (2012).
- [26] J. Becker, D. Brackbill, D. Centola, Network dynamics of social influence in the wisdom of crowds, *Proceedings of the national academy of sciences* **114**, E5070 (2017).
- [27] K. Bhattacharya, T. Vicsek, Collective foraging in heterogeneous landscapes, *Journal of the Royal Society Interface* **11**, 20140674 (2014).
- [28] C. Heins, et al., Collective behavior from surprise minimization, Proceedings of the National Academy of Sciences 121, e2320239121 (2024).
- [29] R. Martínez-García, J. M. Calabrese, T. Mueller, K. A. Olson, C. López, Optimizing the search for resources by sharing information: Mongolian gazelles as a case study, *Physical Review Letters* **110**, 248106 (2013).
- [30] K. Garg, C. T. Kello, P. E. Smaldino, Individual exploration and selective social learning: Balancing exploration–exploitation trade-offs in collective foraging, *Journal of The Royal Society Interface* **19**, 20210915 (2022).
- [31] K. Garg, P. E. Smaldino, C. T. Kello, Evolution of explorative and exploitative search strategies in collective foraging, *Collective Intelligence* **3**, 26339137241228858 (2024).
- [32] K.-I. Goh, A.-L. Barabási, Burstiness and memory in complex systems, *Europhysics Letters* **81**, 48002 (2008).
- [33] U. Hahn, J. U. Hansen, E. J. Olsson, Truth tracking performance of social networks: how connectivity and clustering can make groups less competent, *Synthese* **197**, 1511 (2020).
- [34] R. P. Mann, Collective decision-making under changing social environments among agents adapted to sparse connectivity, *Collective Intelligence* **1**, 26339137221121347 (2022).
- [35] D. M. Gordon, The organization of work in social insect colonies., *Nature* **380** (1996).
- [36] D. M. Gordon, The rewards of restraint in the collective regulation of foraging by harvester ant colonies, *Nature* **498**, 91 (2013).
- [37] D. M. Gordon, The ecology of collective behavior, *PLoS biology* 12, e1001805 (2014).

- [38] I. D. Couzin, J. Krause, N. R. Franks, S. A. Levin, Effective leadership and decision-making in animal groups on the move, *Nature* **433**, 513 (2005).
- [39] C. Torney, Z. Neufeld, I. D. Couzin, Context-dependent interaction leads to emergent search behavior in social aggregates, *Proceedings of the National Academy of Sciences* **106**, 22055 (2009).
- [40] S. B. Rosenthal, C. R. Twomey, A. T. Hartnett, H. S. Wu, I. D. Couzin, Revealing the hidden networks of interaction in mobile animal groups allows prediction of complex behavioral contagion, *Proceedings of the National Academy of Sciences* **112**, 4690 (2015).
- [41] A. J. Ward, D. J. Sumpter, I. D. Couzin, P. J. Hart, J. Krause, Quorum decision-making facilitates information transfer in fish shoals, *Proceedings of the National Academy of Sciences* **105**, 6948 (2008).
- [42] D. Biro, T. Sasaki, S. J. Portugal, Bringing a time–depth perspective to collective animal behaviour, *Trends in ecology & evolution* **31**, 550 (2016).
- [43] N. E. Humphries, *et al.*, Environmental context explains lévy and brownian movement patterns of marine predators, *Nature* **465**, 1066 (2010).
- [44] C. J. Torney, A. Berdahl, I. D. Couzin, Signalling and the evolution of cooperative foraging in dynamic environments, *PLoS computational biology* **7**, e1002194 (2011).
- [45] W. Toyokawa, A. Whalen, K. N. Laland, Social learning strategies regulate the wisdom and madness of interactive crowds, *Nature Human Behaviour* **3**, 183 (2019).
- [46] P. E. Smaldino, C. Moser, A. Perez Velilla, M. Werling, Maintaining transient diversity is a general principle for improving collective problem solving, *Perspectives on Psychological Science* **19**, 454 (2024).
- [47] M. Dumke, M. E. Herberstein, J. M. Schneider, Producers and scroungers: feeding-type composition changes with group size in a socially foraging spider, *Proceedings of the Royal Society B: Biological Sciences* **283**, 20160114 (2016).
- [48] S. Garnier, J. Gautrais, G. Theraulaz, The biological principles of swarm intelligence, *Swarm intelligence* **1**, 3 (2007).
- [49] P. Romanczuk, M. Bär, W. Ebeling, B. Lindner, L. Schimansky-Geier, Active brownian particles: From individual to collective stochastic dynamics, *The European Physical Journal Special Topics* **202**, 1 (2012).

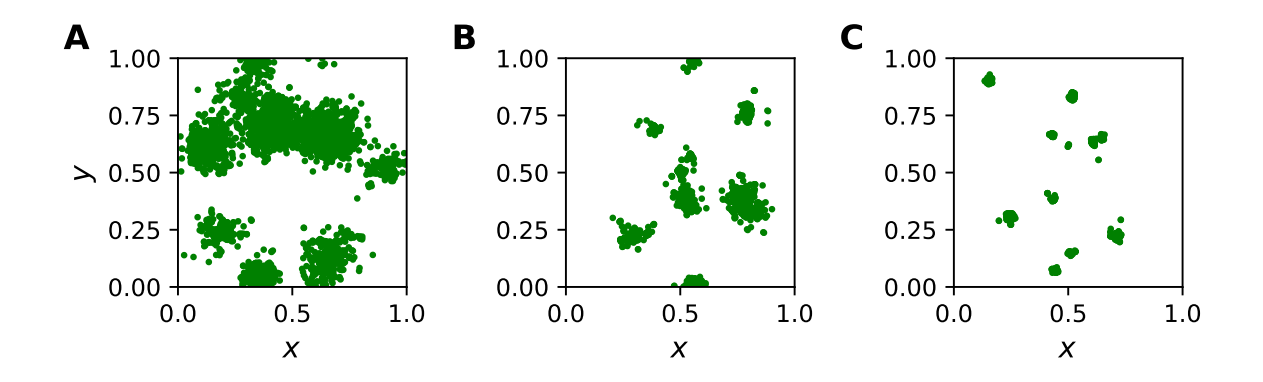
Supplementary Information

Contents

S 1	Target distribution	S 1
S2]	Instantaneous search efficiency over the time	S2
S3 (Group size	S3

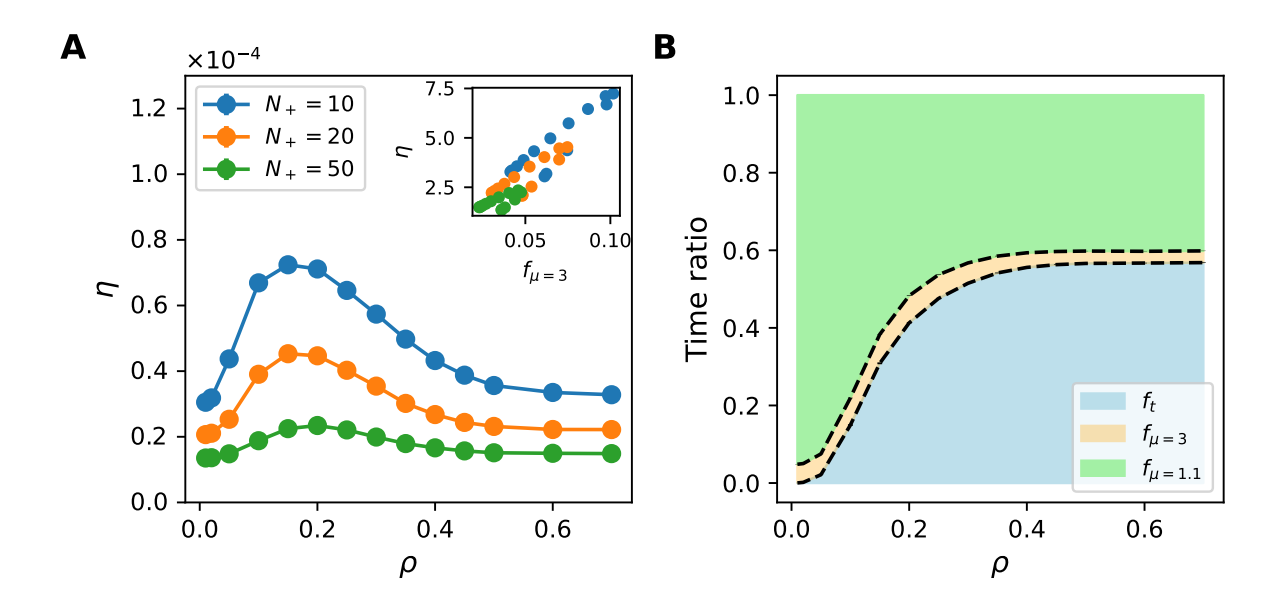
S1 Target distribution

The parameter β controls the spatial distribution of targets around the target seeds, such that $\beta \to 1$ results in a nearly uniform distribution, while $\beta \to 3$ produces a distribution with tightly clustered targets. The main text presents the results using a target distribution with $\beta = 2$. Here, we show results for 50 agents with $\beta = 1.1$ and $\beta = 3$, with the number of patches set to 10, 20, and 50, consistent with the main text.



Supplementary Figure 1: β controls the clustering of targets within a patch (A)(B)(C) The target distributions feature 10 patches of 600 targets each, with varying degrees of clustering controlled by $\beta = 1.1$, $\beta = 2$, and $\beta = 3$.

In the main text, the optimal ρ decreases as N_+ increases when $\beta=2$, because exploring a new patch becomes more important than exploiting a known one in this scenario. This effect is less pronounced when $\beta=1.1$, as targets are scattered more extensively around each patch center. In this scenario, targets are so sparsely distributed that agents need to rely on exploration even within the same patch to collect targets. As a result, the time ratio of exploitation is minimal, while that of exploration increases compared to the case where $\beta=2$. Since agents

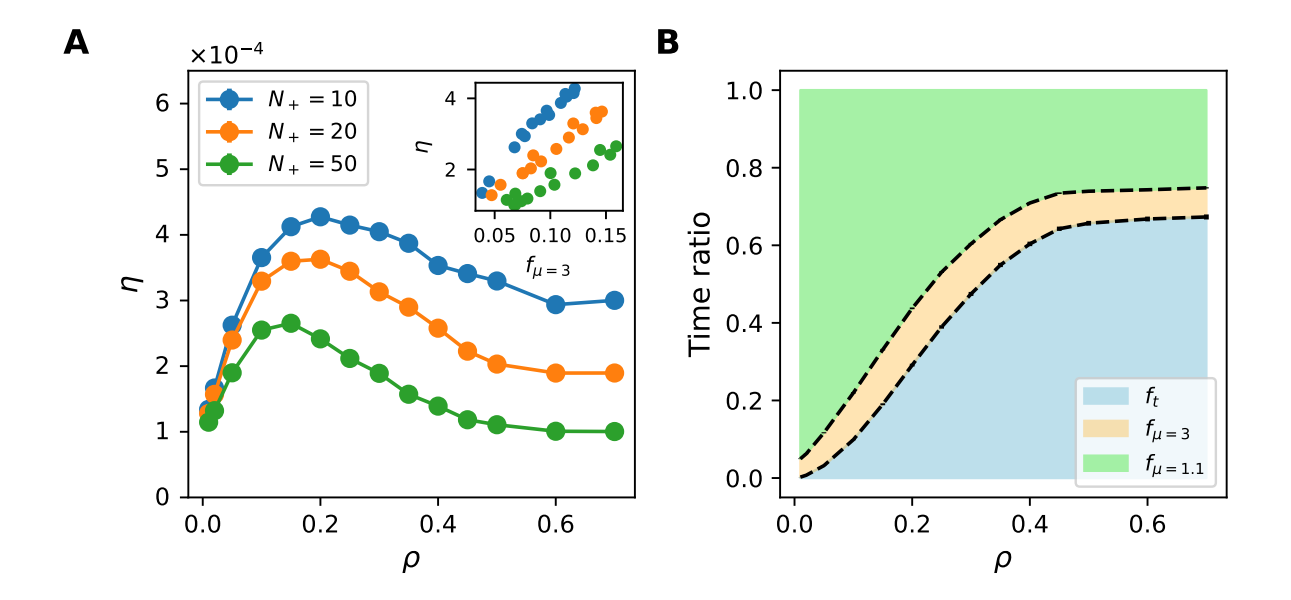


Supplementary Figure 2: Sparsely distributed targets per patch lowers the efficiency and time ratio of exploitation (A) Plots of efficiency as a function of ρ with a fixed number of agents $N_A = 50$ and a series of number of patches, $N_+ = 10$, $N_+ = 20$, and $N_+ = 50$, while the total number of targets within the domain is fixed at 6000. The controlling parameter of the target distribution is $\beta = 1.1$. Error bars indicating 95% confidence interval are too short to show on the figure. The inset shows that efficiency is positively correlated with $f_{\mu=3}$, time ratio of exploitation. (B) Averaged time ratios spending on three behaviors for the case of $N_+ = 20$ in (A) with 50 agents.

already are highly dependent on exploration, the optimal ρ does not decrease significantly as N_+ increases, as shown in Supplementary Fig. 2. Conversely, this effect strengthens when $\beta=3$, where targets are closely clustered around each patch center, making agents more dependent on exploration to find targets in a new patch. Therefore, the optimal ρ decreases significantly as N_+ increases, as shown in Supplementary Fig. 3. For cases with the same number of patches N_+ , the peak efficiency at the optimal ρ increases as β rises from 1.1 to 3. This is because a higher β leads to more tightly clustered targets, which reduces the time needed for agents to deplete a patch of its resources. The efficiency curves with different β values show that our model is more effective for heterogeneously distributed targets than for randomly distributed targets.

S2 Instantaneous search efficiency over the time

Considering the targets can be consumed by agents, the efficiency varies during the search with the number of targets decreased over the time. To show the trends of instantaneous efficiency

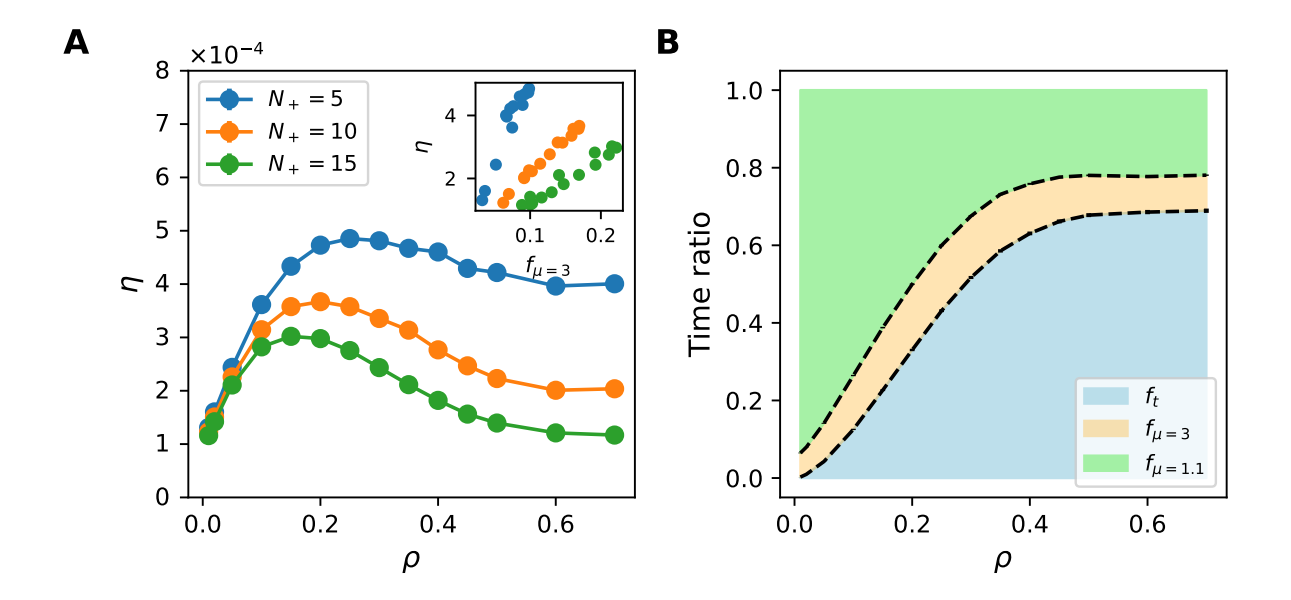


Supplementary Figure 3: Closely distributed targets per patch increases the efficiency and lower the time ratio of exploitation (A) Plots of efficiency as a function of ρ with a fixed number of agents $N_A = 50$ and a series of number of patches, $N_+ = 10$, $N_+ = 20$, and $N_+ = 50$, while the total number of targets within the domain is fixed at 6000. The controlling parameter of the target distribution is $\beta = 3$. Error bars indicating 95% confidence interval are too short to show on the figure. The inset shows that efficiency is positively correlated with $f_{\mu=3}$, time ratio of exploitation. (B) Averaged time ratios spending on three behaviors for the case of $N_+ = 20$ in (A) with 50 agents.

during the search, we compare the efficiency of cases with the same number of targets in each patch as shown in Supplementary Fig. 4. From this figure, we can learn that the normalized efficiency increases due to the decrease in the number of patches. The optimal ρ increases as the number of patches decreases, meaning that agents need more cooperation through social learning as resources become sparse. The optimal ρ still has the maximal time ratios of exploitation in each case. Moreover, the time ratios of exploitation decrease, meaning that exploration becomes more important as the number of patches decreases.

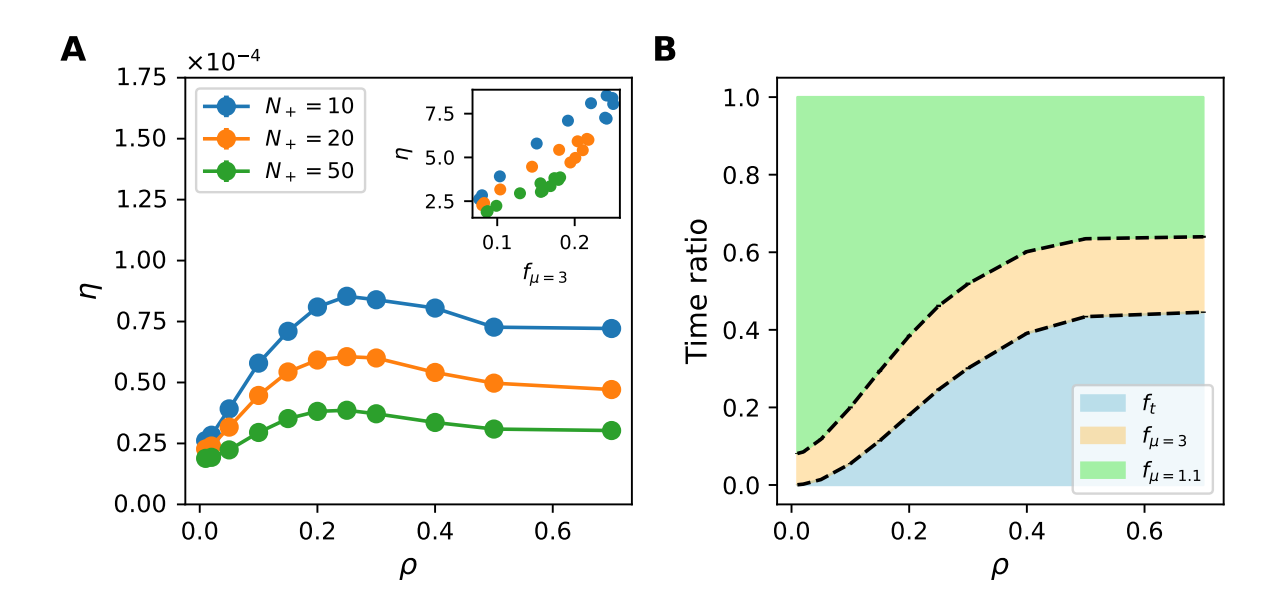
S3 Group size

After testing the case of 10 agents searching for the targets with the same distribution as that in Fig. 2, we can see that the optimal ρ still exists, and it corresponds to the maximal time ratios of exploitation. However, the shape of efficiency curves are flatter compared to cases with 50 agents in the main text. This occurs because the smaller number of agents limits the maximum instantaneous efficiency that can be achieved by social learning and the following tar-



Supplementary Figure 4: The optimal ρ increases as the number of patches decreases (A) Plots of efficiency as a function of ρ with a fixed number of agents $N_A = 50$ and a series of number of patches, $N_+ = 5$, $N_+ = 10$, and $N_+ = 15$, while the number of targets in each patch is fixed and the total numbers of targets are 2500, 5000, and 7500, respectively. The controlling parameter of the target distribution is $\beta = 2$. Error bars indicating 95% confidence interval are too short to show on the figure. The inset shows that efficiency is positively correlated with $f_{\mu=3}$, time ratio of exploitation. (B) Averaged time ratios spending on three behaviors for the case of $N_+ = 10$ in (A) with 50 agents.

geted walk, thereby diminishing the advantages of collective search. As a result, the efficiency curves the efficiency curves show less variation and are less dependent on ρ . This suggests that the model is more effective for larger groups. The group size constraint on instantaneous efficiency also leads agents to use a larger ρ to attract more peers to achieve higher instantaneous efficiency, which, in turn, increases the optimal ρ . Additional videos are available at https://www.youtube.com/playlist?list=PLgRFM9nAjJRwoZvCGBAdCIE-BYNgPmSuV.



Supplementary Figure 5: Smaller group size limited the function of social learning which make efficiency curves fatter (A) Plots of efficiency as a function of ρ with a fixed number of agents $N_A = 10$ and a series of number of patches, $N_+ = 10$, $N_+ = 20$, and $N_+ = 50$, while the total number of targets within the domain is fixed at 6000. The controlling parameter of the target distribution is $\beta = 2$. Error bars indicating 95% confidence interval are too short to show on the figure. The inset shows that efficiency is positively correlated with $f_{\mu=3}$, time ratio of exploitation. (B) Averaged time ratios spending on three behaviors for the case of $N_+ = 20$ in (A).